

Apparent mass of seated man—First determination with a soft seat and dynamic seat pressure distributions

Barbara Hinz^{a,*}, Sebastian Rützel^b, Ralph Blüthner^a, Gerhard Menzel^a,
Horst Peter Wölfel^b, Helmut Seidel^a

^a*Federal Institute for Occupational Safety and Health, Vibration and Electromagnetic Fields Unit,
Nöldnerstr. 40-42, D-10317 Berlin, Germany*

^b*Department of Structural Dynamics, Darmstadt University of Technology, Petersenstr. 30, D-64287 Darmstadt, Germany*

Received 2 May 2006; received in revised form 10 May 2006; accepted 8 June 2006
Available online 1 August 2006

Abstract

Data of the impedance and/or the apparent mass of the sitting human body during the exposure to whole-body vibration in z -direction using rigid seats were standardized in the ISO 5982. These data are available as target functions for model developments. Models developed on this data basis should also apply to driver seats with a soft seat and backrest cushion, although the qualitative different contact conditions were neglected. Due to insufficient technical prerequisites, the determination of forces at the interface between subject and soft seat was impossible until very recently. Results of studies during static conditions showed clear differences in the pressure distributions between the rigid and the soft contact areas. In this experimental study pressure distributions on a seat cushion were measured during whole-body vibration in z -direction (random signal in the frequency range between 0.3 and 20 Hz, vibration magnitudes 0.25, 0.8, and 1.6 m s^{-2} unweighted root mean square measured at the seat base) with a sampling rate of 32 ms. The apparent masses were calculated by the forces derived from the pressure distributions and accelerations measured at one point of the seat cushion near the buttocks. The moduli of the apparent masses derived for the soft seat were clearly lower than those determined for a rigid seat. These apparent masses showed a similar dependence on the vibration magnitude as the apparent mass functions derived in the usual way for rigid seats. Factors that could explain differences between the apparent mass functions derived for the soft and rigid seat were discussed and evaluated. The data of this study indicate the possibility and necessity to consider the contact conditions at the interface when deriving target functions for the model development. Recommendations for technical improvements and further experimental studies with driver seats were derived.

© 2006 Elsevier Ltd. All rights reserved.

1. Introduction

Numerous studies about the impedance and/or apparent mass of the seated human body in z -direction using rigid seats were published [1–10]. To get target functions for the model developments the present stage of the knowledge was summarized in the ISO 5982 [1]. At present mathematical models and dummies are developed

*Corresponding author. Tel.: +49 30 51548 4431; fax: +49 30 515484170.

E-mail address: hinz.barbara@baua.bund.de (B. Hinz).

by an approximation of their apparent mass to the idealized values published in the ISO 5982 [1] or averaged apparent mass functions of subjects (e.g. [11]) measured on rigid seats.

The dependence of the apparent mass function on the postures was tested for conditions with and without backrest contact as well as with hands in lap or on supports, e.g. steering wheels [4]. Toward [10] summarized that a support of the back caused higher resonance frequencies and slightly lower maximum moduli of the apparent mass for subjects sitting on a horizontal plane. Mansfield and Maeda [12] registered similar results of the apparent mass for the ‘back-on’ and ‘back off’ condition for many subjects. With contact to a soft backrest in an automotive posture [13] the peak frequencies of the apparent mass functions were clearly higher and the normalized maximum moduli were lower than without backrest contact sitting on a horizontal seat plate [14].

The influence of the hand position on the apparent mass response of seated subjects has not been clearly reported in the literature. Rakheja et al. [9] found in a typical automotive posture for the condition ‘hands on steering wheel’ lower maximum moduli of the apparent mass at lower frequencies than for the condition ‘hands in lap’. Wang et al. [15] described that the effect of magnitude of excitation on the apparent mass function was observed to be slightly lower for the condition ‘hands at a steering wheel’ during a typical automotive posture.

Nawayseh and Griffin [16] derived the effects of different contact conditions between buttocks, thighs and a rigid seat plate on the apparent mass function. The peak frequencies depended on the vibration magnitude and the kind of contact with the rigid seat. The peak frequencies were lower with the minimum thigh contact than with the maximum thigh contact during an exposure with 0.125 m s^{-2} root mean square (rms). During vibration magnitudes of 0.250 m s^{-2} rms and 0.625 m s^{-2} rms the effect of the contact conditions on the peak frequencies were unclear, but with a vibration magnitude of 1.25 m s^{-2} rms the peak frequencies were lower during the maximum thigh contact.

The characteristics of the contact areas between the seat cushion and the subject were investigated under static conditions with different techniques since the end of the sixties [17, Table 1]. The pressure distributions under static conditions were clearly different for rigid and soft seat surfaces [18, Fig. 8]. The mean pressure distributions of 23 male subjects show narrow peaks in the range of the buttocks with very low values beneath the thighs for the rigid seat [17, Fig. 4]. For soft seats with a nearly upright backrest the maximum pressure values were clearly lower and distributed in a wider area [17]. The mean value of the total forces supported by a soft seat amounted to 325 N and the mean forces acting perpendicular on the backrest amounted to 65 N [18, Fig. 2]. Both values increased for car seats due to the inclination of the seat surface and the backrest and the lower contact force beneath the feet. Depending on the seat design the mean values of the forces at the seat interface varied around 450 N and at the backrest around 140 N [18].

Results concerning the effect of whole body vibration on the dynamic pressure distributions were published by Wu et al. only [19]. The authors tested the influence of vibration magnitude, frequency, posture, and seat height on the pressure and the force in the range of the buttocks (area $12.25 \text{ cm} \times 24.25 \text{ cm}$) with three male subjects sitting on a rigid seat with a rigid backrest. But the authors could not derive total forces at the seat interface due to the selection of one part of the total contact area.

First measurements of pressure distribution with a low sampling frequency underlined the necessity to derive the forces from the pressure distribution, but the results remain still inadequate [13].

Present models or vibration dummies are based on data registered in studies using a rigid seat. The users of such models expect a simulation of the vibration behaviour of the human body sitting on driver (soft) seats, too. But during practical tests, differences in the frequency responses between subjects and models were obvious. The reasons of these differences remained unclear up to now.

The aim of this experimental study is to derive the apparent mass functions based on the measurement of pressure distributions and the determination of total forces during vibration exposures in z -direction.

2. Methods

2.1. Exposure

Control signals with three magnitudes were generated by the control system of the hexapod simulator as random signals in the range between 0.3 and 20 Hz. Up to 10 steps of iteration were required for each of the

three intensities in order to minimize the error between the desired and produced acceleration in the time domain. The requirements of ISO 13090 [20] were considered. The unweighted rms values in the z -direction at the seat base amounted to 0.25 m s^{-2} (E1), 0.8 m s^{-2} (E2), and 1.6 m s^{-2} (E3) rms. The power spectral densities (PSD) for 13 subjects are shown in Fig. 1. The duration of each exposure was 65 s. The subjects were exposed to the vibration signals according to a balanced sequence.

The functions of the hexapod simulator and of all measuring systems were controlled by a synchronization system, which started the measuring systems and the exposure at a defined point in time. During the measuring period the synchronization system controls sampling by the measuring systems with an external clock rate.

2.2. Subjects

A total of 13 male subjects with body masses between 62.2 and 103.6 kg and body heights between 174 and 196 cm were chosen for tests with a soft and a rigid seat. The individual body masses and body heights are listed in Table 1. Additionally, anthropometric measurements were performed by only one expert with 36 anthropometrical parameters (heights, breadths, depths, and circumferences) measured for each subject in the standing and sitting posture and using anthropological instruments (Siber Hegner Maschinen AG) [21]. The maximum hip breadth in the seating posture varied between 35.3 and 42.0 cm.

2.3. Seats and data acquisition

2.3.1. Soft seat

One experimental test was performed using a soft seat surface. The upper part of a driver seat with an integrated backrest, but without the suspension system was mounted on a rigid plate (Fig. 2). The central part of the seat cushion was horizontal, the lateral sections had an angle of inclination of 12° , the frontal section had an angle of inclination of 10° , and the curved lower part of the backrest cushion had an inclination between 17° and 28° . The subjects sat on the soft seat cushion in a relaxed upright posture with hands on a support and with a backrest-contact restricted to the lumbar region (Fig. 2). Due to safety aspects a seat belt was used. The subjects were instructed to contact the backrest in the lumbar region only. No instruction was given concerning the muscular effort to perform this contact.

At the seat cushion the accelerations were registered by the three dimensional accelerometer ENDEVCO 65–100 in a rubber pad (amplitude response 1–1000 Hz, uncertainty $\pm 5.0\%$) fixed at the seat cushion near the ischial tuberosities. The unweighted rms values of the acceleration in z -direction were 0.23 m s^{-2} for E1, 0.763 m s^{-2} for E2, and 1.37 m s^{-2} for E3. The PSD of the accelerations are shown in Fig. 1. The accelerations at the seat basis were measured by three accelerometers ENDEVCO 7290A-10 Microtron (capacitive sensors, 10 g, 200 mV g^{-1} , 0–500 Hz, uncertainty $\pm 5.0\%$) mounted at an ENDEVCO 7990 block fixed at the rigid plate. The data acquisition was performed by a WaveBook 516 with WBK16 (Iotech).

The pressure distributions at the seat cushion were registered by a pliance system (novel gmbh) composed of the following parts: (1) A sensor mat with 16×16 sensors with sensor areas of 6 cm^2 was selected to register the pressure distributions with a maximum sampling rate. The sensors can register loads acting perpendicularly to the surface of the sensor. (2) The analyzer pliance FTM 017 for the data acquisition. (3) The novel software allows to observe the data registration in frames during the vibration.

The calibration of the sensor mat was performed in a ‘trublu’ calibration device suited for the sensor mat used (novel gmbh, uncertainty $\pm 5.0\%$) together with a digital manometer (Greisinger electronic). The device consists of a rubber membrane, housed within a secure unit. Compressed air is fed into the device thus exerting a pressure on the inserted mat or sensor. The sensor mat is placed within a synthetic leather cover. The mat was loaded in the range between 0.1 and 6 N cm^{-2} with increasing and decreasing pressures on all sensors simultaneously according to the producer manual. Deviations were registered between loading and unloading only during pressures above 4 N cm^{-2} , i.e. outside the range used for the measurements in this study. The calibration was tested by measurements in the calibration device.

A function integrity check was performed daily before the start of experiments in order to check the accuracy of the total force measurements. The body weight of one person (560 N) was measured by scales. Then this person was sitting on the sensor mat for at least 3–4 min to avoid different temperatures of the

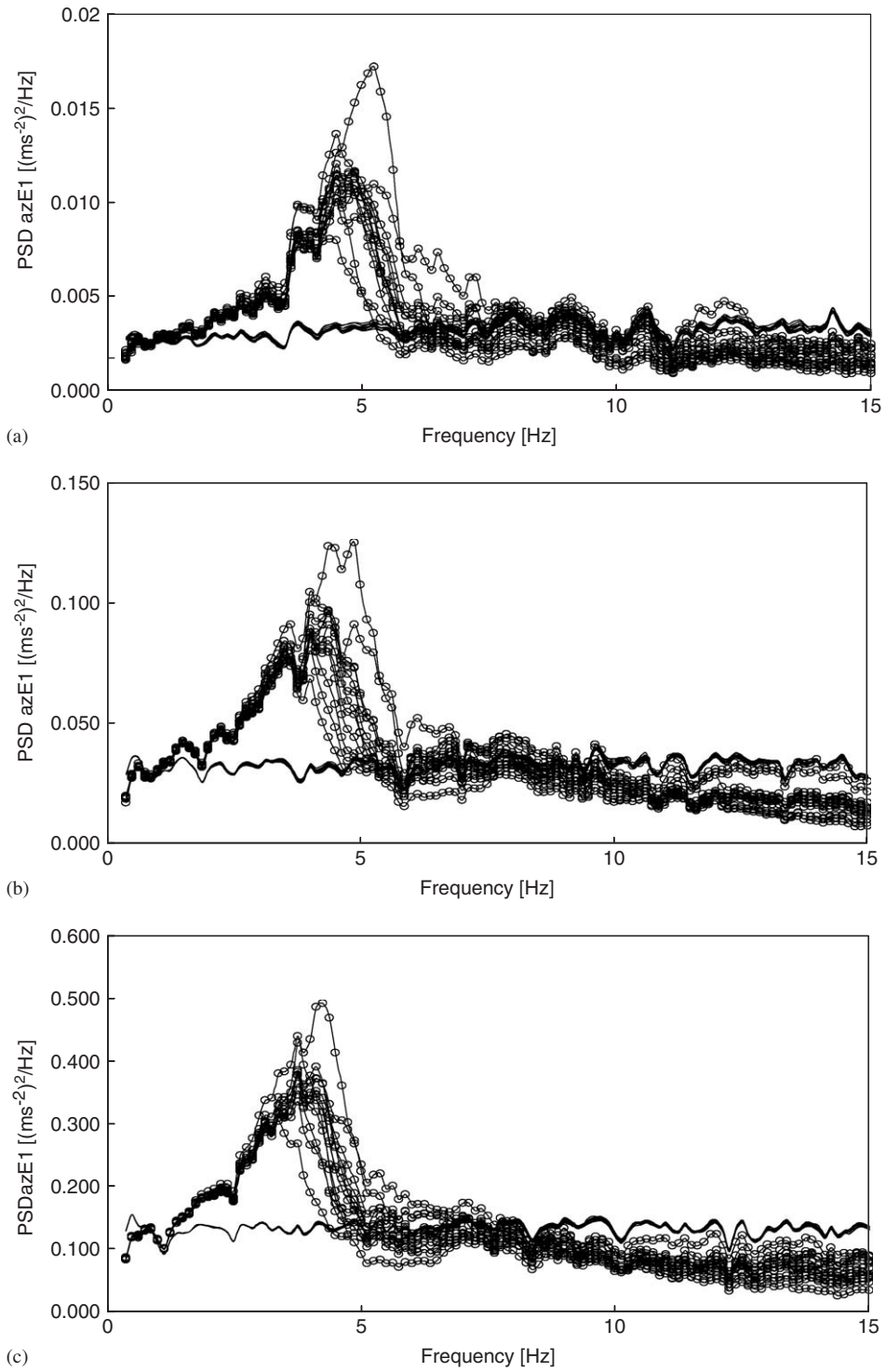


Fig. 1. Individual values of power spectral densities (PSD) of input accelerations (az) measured in z -direction: (a) during the vibration magnitude E1, (b) during the vibration magnitude E2, (c) during the vibration magnitude E3. — input accelerations measured at the seat basis, \bigcirc — input accelerations measured at the seat cushion.

Table 1
Body masses and body heights of the subjects chosen for the experimental study

Subject no.	Body mass (kg)	Body height (cm)
01	76.2	189
02	86.8	183
03	86.6	188
04	70.3	183
05	75.8	192
06	103.6	193
07	100.3	196
08	89	176
09	69.9	182
10	74.4	178
11	71.1	178
12	62.9	174
13	79.0	186

subject and the sensor mat. A zero measurement was performed with an unloaded mat, thereafter the person was sitting down without floor contact of the feet and without backrest contact of the upper body, i.e. the whole body mass resting on the mat. The comparison of the results obtained during the function integrity checks for the whole body mass showed differences between the two methods in the range from 1% to 4%. The warming up procedure was performed for each subject before the tests started. The zero-measurements were performed before each exposure. During the exposure time of 65 s a time dependent shift of pressure measurements was not observed.

For each vibration exposure 1812 frames were registered during 58 s. One frame corresponded to a total sensor area of 1536 cm² (length of each side of the mat 39.19 cm). The external clock rate was 32 m s; the time per frame was 25.6 m s followed by an interval of 6.4 m s until the start of the next frame. The threshold value for the registration of pressure was 0.03 N cm⁻². The resulting forces FZ were derived from the sum of the pressure value times the sum of area of all loaded sensors for each frame. For each frame the maximum peak pressure value was determined.

2.3.2. Rigid seat

Another experimental test was performed using a rigid seat without backrest [cf. 14]. A force plate (Kistler 9396 AB, maximum uncertainty $\pm 4.0\%$) capable of measuring forces in three directions simultaneously was mounted as seat surface in order to measure forces in the vertical (z) direction. The force plate (60 × 40 × 20 cm) consisted of four tri-axial quartz piezoelectric transducers of the same sensitivity located at the corners of the plate. Signals from the force plate were amplified using an eight channel amplifier (Kistler 9865B). The time series of forces were corrected by subtracting the product of the weight of the plate and the actual acceleration. The subjects sat on the force plate, which was integrated in a rigid seat with the hands on a support [14, Fig. 2]. They were exposed to a random signal at three intensities (I1: 0.26 m s⁻²; I2: 0.83 m s⁻²; I3: 1.57 m s⁻² unweighted rms) in the frequency range between 0.3 and 20 Hz.

Accelerations in three translational directions (x , y , and z) were measured at the force plate in each test using three capacitance accelerometers (ENDEVCO 7290A-10, uncertainty $\pm 5\%$ in the range between 0 and 15 Hz) mounted at a special block for these accelerometers (ENDEVCO 7990 block). The data acquisition was performed by a WaveBook 516 with WBK16 (Iotech).

2.4. Motion analysis

A motion analysis system (Qualysis) was used to obtain the individual postures during the experimental tests with the rigid and with the soft seat. The markers were fixed at the acromial joint of the shoulder, at the elbow, wrist and at the hip joint, knee joint and ankle. The time per frame was 50 m s, totally 1520 frames were registered. Two joint points were connected by a straight line with the assumption that the body part between

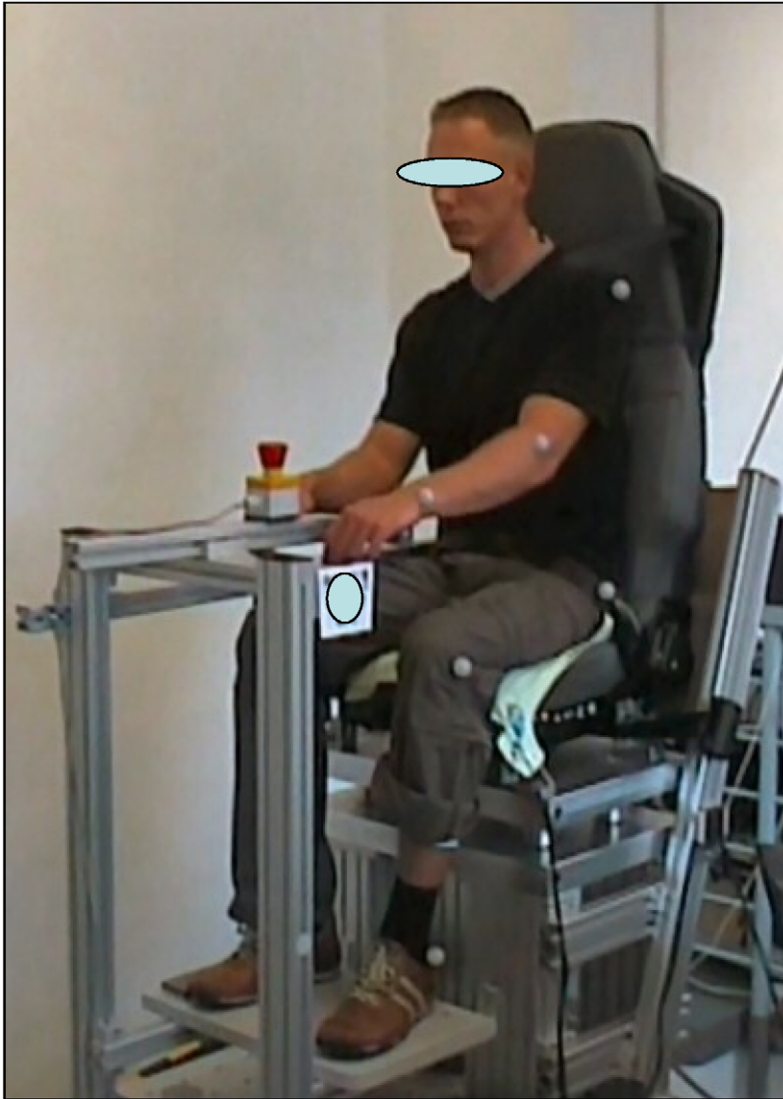


Fig. 2. The experimental situation is illustrated by the photography of a male subject sitting on the seat with the sensor mat.

the joints moves in a similar way as a rigid body between the joint points. Body angles can be calculated between two lines or one line and the horizontal. To compare the mean values of the coordinates of joint points stick figures were calculated.

2.5. Data analysis and statistics

The seat transfer functions were calculated by dividing the cross-spectral density function between the acceleration at the seat base and the acceleration measured at the interface between the subject and the seat cushion by the power spectral density of the acceleration at the seat base.

The apparent mass (AM) is defined as the complex ratio of force amplitude (FZ) and acceleration amplitude (a). The apparent mass was calculated by the cross spectral density method using a MatLab routine.

$$AM(f) = \frac{FZ(f)}{a(f)}. \quad (1)$$

The associated coherency was calculated as

$$\gamma^2(FZa) \equiv \frac{|FZa(f)|^2}{FZ(f)a(f)}. \quad (2)$$

The influence of the factor vibration magnitude on the maxima of the moduli of the apparent masses and their frequencies was tested by the general linear model (GLM) Repeated Measures procedure (SPSS PC—analysis of variance, when the same measurement is made several times on the same subject). The GLM Repeated Measures procedure provides both univariate and multivariate analysis including the Bonferroni post hoc test. The Bonferroni test, based on Student's statistic, adjusts the observed significance level for the fact that multiple comparisons of mean values are made.

3. Results

3.1. Pressure distributions

The pressure distributions can be described by the resulting forces FZ (Fig. 3(a) and (d)), the loaded areas (Fig. 3(b) and (e)), and the pressure values (Fig. 3(c) and (f)). The mean values of all three parameters show a tendency to increase with the vibration magnitude (Fig. 3(a)–(c)). The maximum values of the force FZ (Fig. 3(d)) and the maximum pressure values (Fig. 3(f)) depend clearly on the vibration magnitude. The maximum loaded area tends also to higher values with the increased vibration magnitude.

3.2. Seat transfer function

The individual magnitudes and phases of the transfer functions are shown in Fig. 4. Values below 1 at the frequencies below 1 Hz were caused by the limited amplitude response of the accelerometer used. The maximum amplification of the input acceleration was registered between 4 and 5 Hz with lower frequencies at the higher intensities (Fig. 4(a)–(c)). The accelerations at the seat cushion were higher than the input accelerations by factors between 1.5 and 2 in this frequency range. Further peaks in the range between 8 and 10 Hz were detectable in the curves of the magnitudes. These peak values amounted between 0.8 and 1.2 and contribute to the amplification of the seat signal to a lower extent. The mean values of the magnitudes and phases of the transfer functions (Fig. 5) shifted to the lower frequencies if the vibration magnitude increased from E1 to E3. The second peak appeared in the mean values of magnitudes of the transfer function more clearly during E1 than during E2 and E3.

3.3. Apparent masses

3.3.1. Soft seat

The individual curves of the moduli of the apparent mass illustrate the ranges of the interindividual variability (Fig. 6). The variability decreased with the vibration magnitude at higher frequencies. Relatively small differences were registered between the apparent masses of the 13 subjects at frequencies above 10 Hz. To quantify the extent of the variability of the moduli of the apparent mass, the standard deviation was selected and calculated for each bandwidth. A remarkable variation occurred in the range of the main peak between 3 and 6 Hz (Fig. 7(b)). The maximum standard deviations were lower with the increased vibration magnitude and occurred at lower frequencies. One reason for the differences between the subjects is the variability of the body stature.

Two peaks of the moduli of the apparent mass were registered: the main peak (Peak 1) with moduli between 33.66 and 74.09 kg in the frequency range between 3.5 and 6.25 Hz (Table 2), and a second peak (Peak 2) with moduli between 19.17 and 39.65 kg in the frequency range between 6.75 and 12.25 Hz. The mean values of the moduli of the apparent masses shifted to the lower frequencies with the increasing vibration magnitude (Fig. 7(a)). The values of the individual coherency functions (Fig. 8) were found between 0.8 and 1.0 during the exposures E2 and E3 in the frequency range from 0.5 to 12 Hz. During the exposure E1 the variation between the subjects is high in the frequency range above 5 Hz.

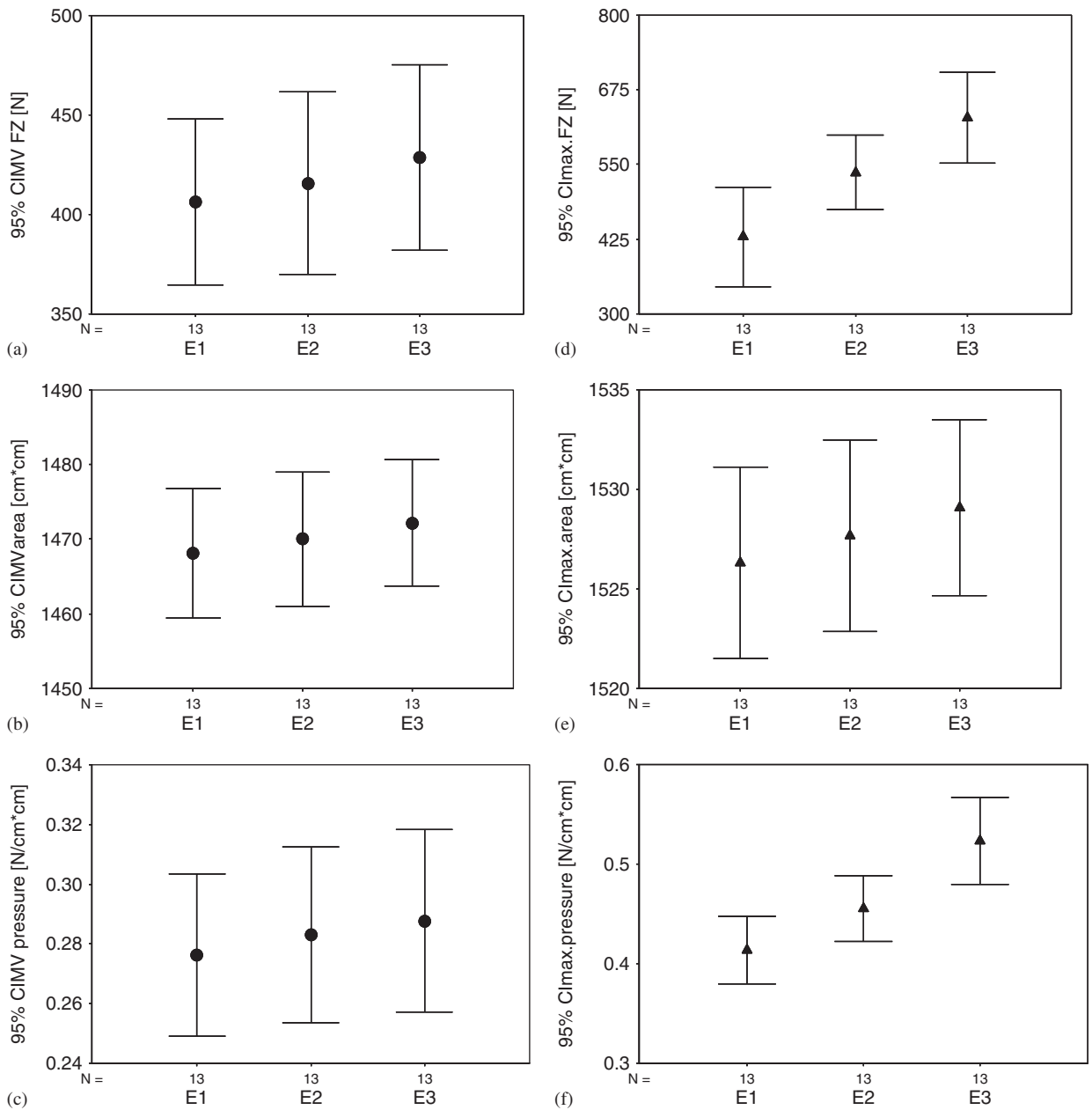


Fig. 3. Mean values (MV) and 95% confidence interval (CI) of the parameters derived from the pressure distributions measured during the vibration magnitudes E1, E2, and E3: (a) the mean resulting forces FZ , (b) the mean loaded areas, (c) the mean pressure values, (d) the maximum resulting forces FZ , (e) the maximum loaded areas, (f) the maximum pressure values.

The effects of the factor vibration magnitude on the peak moduli and the peak frequencies of the apparent mass were tested for both main peaks. The multivariate analysis shows a significant effect (significance level $p < 0.05$) of the vibration magnitude on the parameter characterizing the two peaks. The univariate tests provided the influence of the vibration magnitude on the peak moduli of the first peak and on the peak frequencies of the first and the second peak. The vibration magnitude did not effect the moduli of the second peak. The results of the Bonferroni post hoc tests showed, that the mean peak frequencies of both peaks were

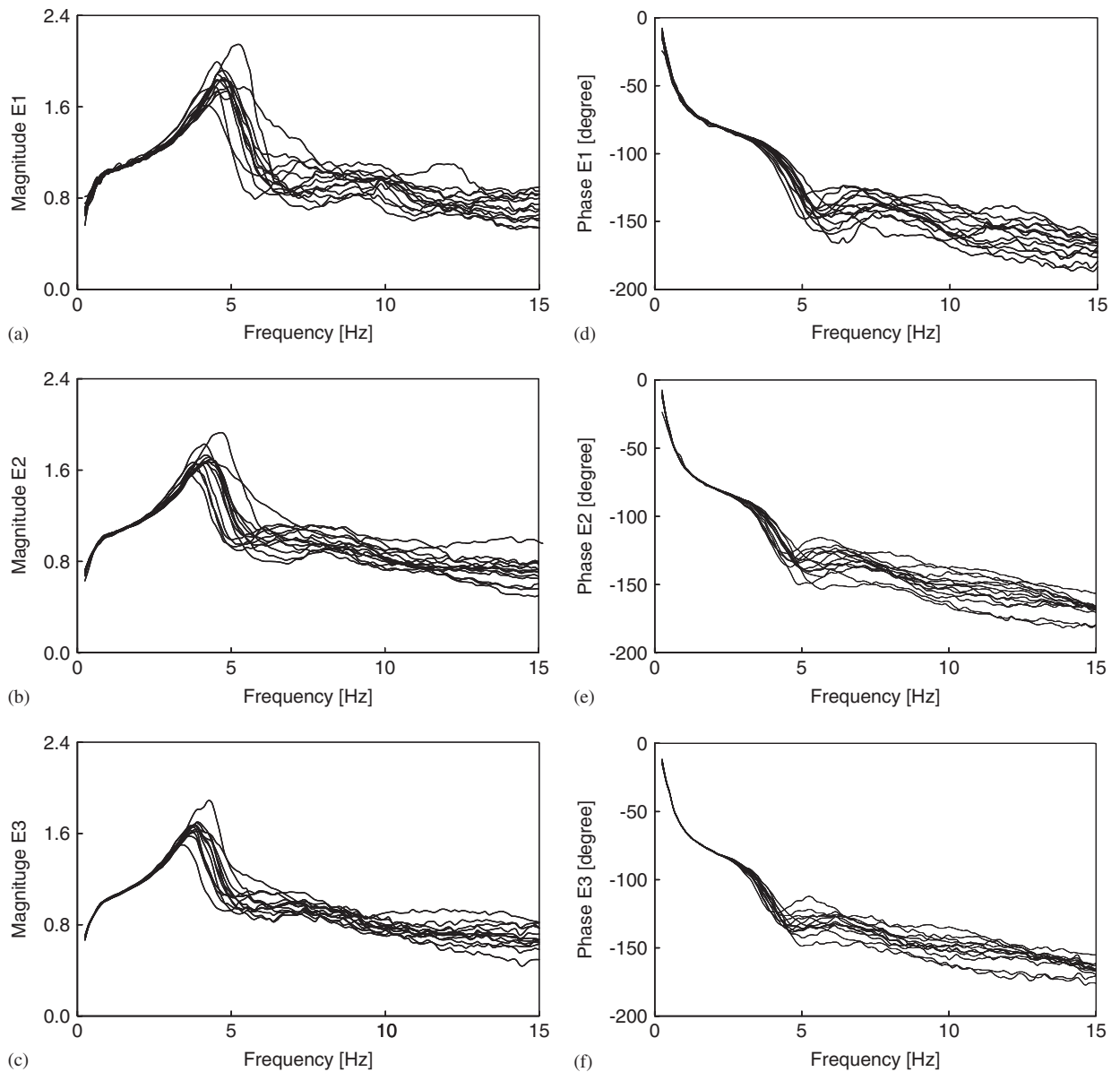


Fig. 4. Individual transfer functions between the accelerations in z -direction measured at the seat basis and at the seat cushion: (a) magnitudes during the vibration magnitude E1, (b) magnitudes during the vibration magnitude E2, (c) magnitudes during the vibration magnitude E3, (d) phases during the vibration magnitude E1, (e) phases during the vibration magnitude E2, (f) phases during the vibration magnitude E3.

significantly lower with the increasing vibration magnitudes tested (Table 3). The mean peak moduli of the first peak were significantly different between E1 and E3 only.

The moduli of the apparent mass for subjects sitting on the soft seat (AMS) were normalized by the share of body mass supported by the soft seat according to column 3 (Soft seat, forces seat cushion) of Table 4. The mean values of AMS are presented in Fig. 9.

The results of the motion analysis show small differences within the body angles of one subject (Fig. 10(a)) during all conditions tested, but the ranges between the body angles varied to a higher extent between all subjects (Fig. 10(b)). The differences between the individual postures of the subjects with the minimum and maximum body mass and body height are illustrated in Fig. 10(c) and (d), respectively.

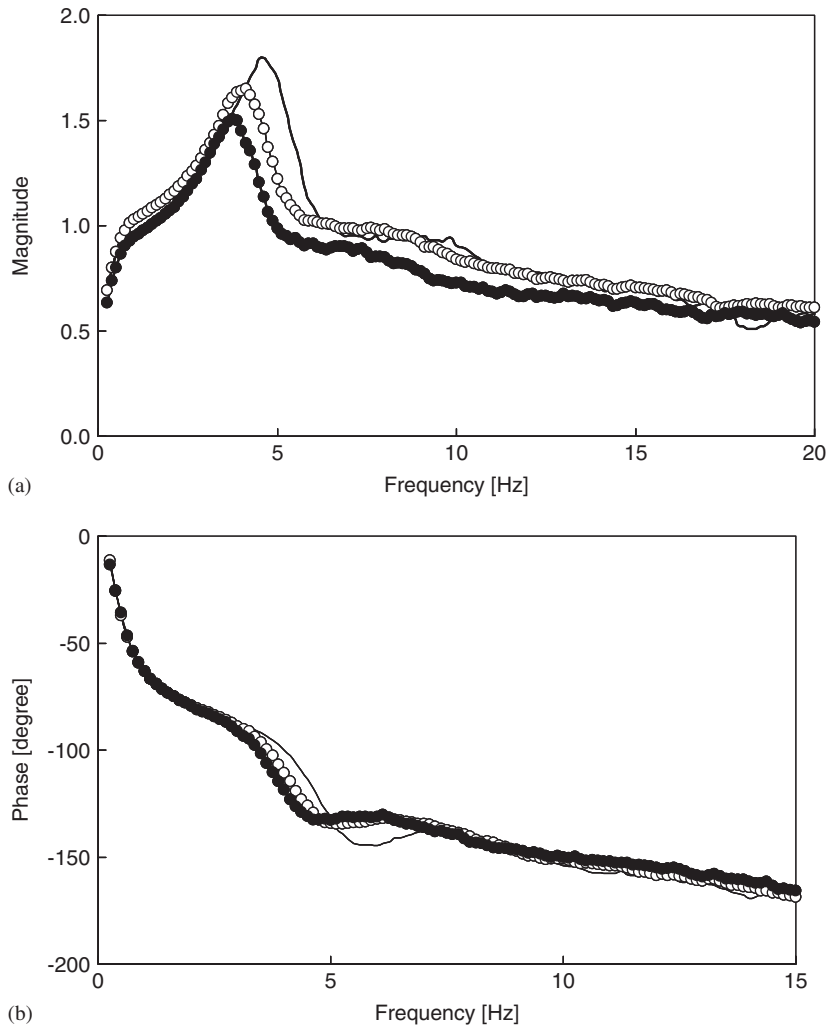


Fig. 5. Mean transfer functions between the accelerations in z -direction measured at the seat basis and the seat cushion: (a) mean magnitudes, (b) mean phases. — during the vibration magnitude E1, ○ during the vibration magnitude E2, ● during the vibration magnitude E3.

3.3.2. Rigid seat

A remarkable variability was registered for the individual values of the apparent masses [14]. The extent of this variability is described by the standard deviations (Fig. 11(b)). The maximum values of the standard deviations occurred in the range between 3 and 7 Hz corresponding to the maximum values of the moduli of the apparent masses (Fig. 11(a)). The variability decreased at higher frequencies and reached the minimum values above 10 Hz, with the lowest values during the highest vibration magnitude I3. One main peak was identified for all subjects with moduli between 68.58 and 145.70 kg in the frequency range between 3.25 and 6.63 Hz (Table 5). A second peak was detectable in the individual curves in the frequency range between 6.50 and 10.57 Hz (Table 5). The mean values of the apparent masses shifted towards lower frequencies with the increasing vibration magnitude (Fig. 11(a)). The effects of the factor vibration magnitude on the peak moduli and peak frequencies of the apparent mass were tested for the main peak. The multivariate analysis shows a significant effect (significance level $p < 0.05$) of the vibration magnitude on the parameters characterising the main peak. The univariate tests reflected a significant influence of the factor vibration on the peak frequency only. The peak frequencies were significantly lower with the increasing intensity (Table 3).

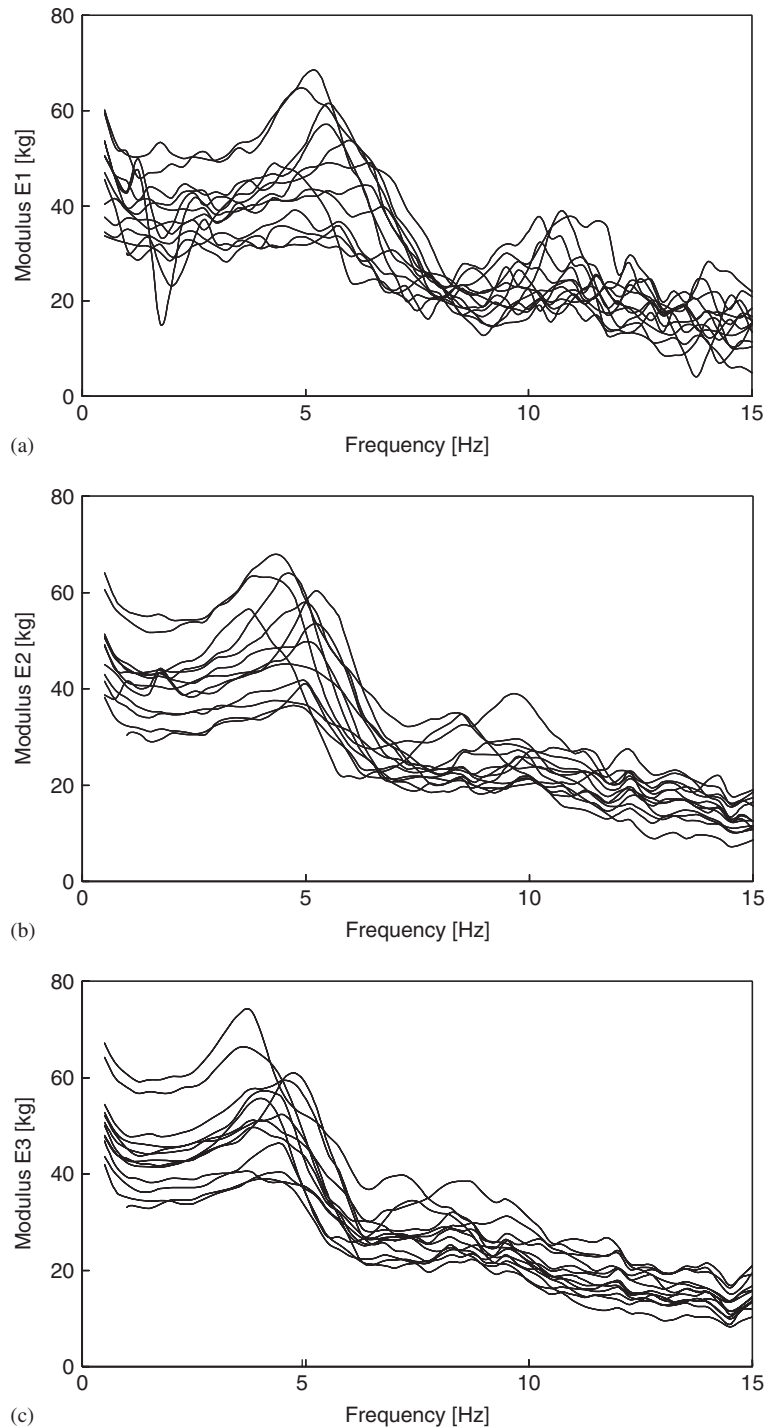


Fig. 6. Individual values of the moduli of the apparent mass functions calculated by the forces derived from pressure distributions and accelerations measured at the seat cushion: (a) during the vibration magnitude E1, (b) during the vibration magnitude E2, (c) during the vibration magnitude E3.

The moduli of the apparent mass for subjects sitting on a rigid seat (AMR) were normalized by the body mass supported by the rigid seat plate according column 4 (Rigid seat, forces seat plate) of Table 4. The mean values of the normalized AMR are shown in Fig. 9.

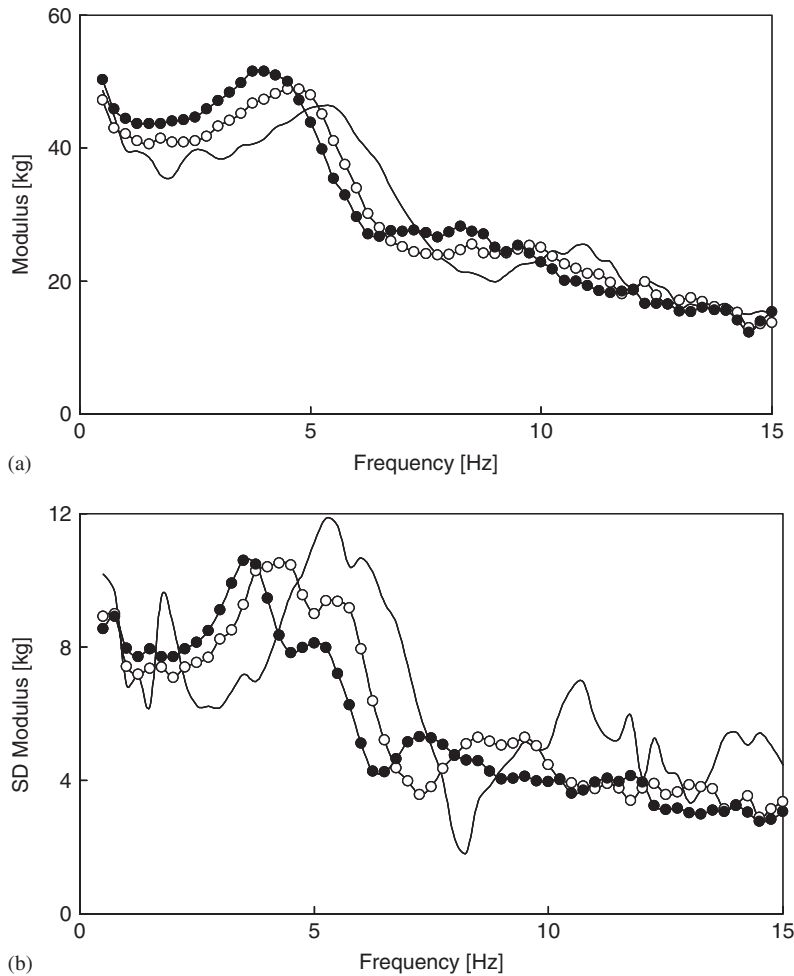


Fig. 7. Moduli of the apparent mass functions calculated by the forces derived from pressure distributions and the accelerations measured at the seat cushion: (a) mean moduli, (b) standard deviations. — during the vibration magnitude E1, ○ during the vibration magnitude E2, ● during the vibration magnitude E3.

4. Discussion

4.1. Critique of the methodology

The methods employed in the present study require careful consideration. The vertical force acting on the seat cushion was on average 180 N smaller than that acting on the rigid seat. Assuming a significant friction between the body and the backrest, a considerable part of body mass above the seat was most likely supported by the backrest. On average, the vertical force acting on the seat cushion (with use of backrest) was 180 N lower than the vertical force acting on the rigid seat (without use of backrest). With a backrest angle of 28° , 180 N could cause up to 84.5 N acting perpendicular on the mat placed on the backrest. With an average backrest angle of 22.5° , up to 69 N would result. On average, FX of 85 N was measured on the backrest in another study with the same subjects and seat [22], i.e., the measurement was near the order of magnitude that can be expected. The force FX acting on the backrest comprises two components—a passive force resulting from the weight of the body leaning against the backrest, and an active force resulting from uncontrolled muscle activity to achieve the required contact with the backrest. The latter component can also modify the friction between the body and the backrest.

Table 2

Minimum, maximum, mean values, and standard deviations (SD) for the peak moduli ($\max.|AM|$ [kg]) and peak frequencies ($f(\max.|AM|)$ [Hz]) of the apparent mass functions during the vibration magnitudes E1, E2, and E3

	Minimum	Maximum	Mean	SD
<i>Peak 1</i>				
E1 $\max. AM $	33.66	68.24	48.98	11.34
E2 $\max. AM $	36.47	67.78	51.87	10.69
E3 $\max. AM $	38.91	74.09	53.29	10.53
E1 $f(\max. AM)$	4.25	6.25	5.25	0.58
E2 $f(\max. AM)$	3.75	5.25	4.65	0.48
E3 $f(\max. AM)$	3.5	4.75	4.08	0.36
<i>Peak 2</i>				
E1 $\max. AM $	19.17	38.97	28.94	6.35
E2 $\max. AM $	21.34	38.90	28.07	5.39
E3 $\max. AM $	22.73	39.65	29.77	5.15
E1 $f(\max. AM)$	8.75	12.25	10.48	0.89
E2 $f(\max. AM)$	8.25	10.50	9.48	0.76
E3 $f(\max. AM)$	6.75	9.5	8.32	0.79

The data acquisition and data processing of the pressure distributions indicated some limitations of this first experimental study concerning this issue. The sensor size of 6 cm^2 delivered a relatively rough scanning of the pressure distribution. Based on a comparison of the length of each side of the sensor mat (39.19 cm) and the range of hip breadth of the subjects (35.3 and 42.0 cm), detailed inspections of the sensor rows at the edges were performed. In contrast to static tests with larger sensor mats (length of each side 45.25 cm [23]), clearly higher values (between 36.4 and 88.0 N) were registered at the left, right and rear edges. Depending on the hip breadth of the subjects one may assume that up to one sensor row at these edges was lost, which corresponds to a range up to 10% of the body weight. This shortcoming may have led to an underestimation of the apparent mass function to a certain extent. Smaller sensor sizes together with a larger sensor area are important prerequisites for a more precise registration of the static forces.

The present maximum sampling rate of 31.25 Hz required a threshold value of 0.03 m s^{-2} in order to avoid fluttering of sensors [24]. Hence, the apparently “unloaded” area of the mat could have been loaded below this threshold. The unloaded area amounted on average to 14% of the total area. Therefore, the possible error caused by this threshold ranged from 0 to about 5.5 N. Higher sampling rates would allow a lower threshold value and the calculation of the apparent mass function up to higher frequencies.

Further, it should be considered that the flexible sensor mat can only sample pressure perpendicular to the local contact surface, and the measured total contact force is a summation of the contact forces at various locations. Therefore, the measured total contact force is smaller than the vertical load when a subject is sitting on a driver seat. The inclinations of the peripheral areas of the otherwise horizontal seat cushion used were in the range between 10° and 12° . In these areas the measured forces can be lower than the vertical forces by a factor of about 0.98 depending of the individual contact area of the subjects.

During the experiments the acceleration was measured as usual at one point in the region between the buttocks. But an additional test delivered different PSD of the accelerations measured beneath the left thigh and measured between the buttocks. As expected the maximum of the PSD of the acceleration measured between the buttocks occurred around 4 Hz, whereas the maximum of the PSD of the acceleration measured beneath the thigh appeared around 8 Hz. Based on this result, the accelerations might be measured at several points of the human–seat interface and related to corresponding forces in future experimental studies.

4.2. Factors affecting the apparent mass

4.2.1. Vibration magnitude

To the author’s knowledge, data of the apparent mass functions derived from measurements on soft seats have not been published up to now, but data obtained with rigid seats can be compared with the essential

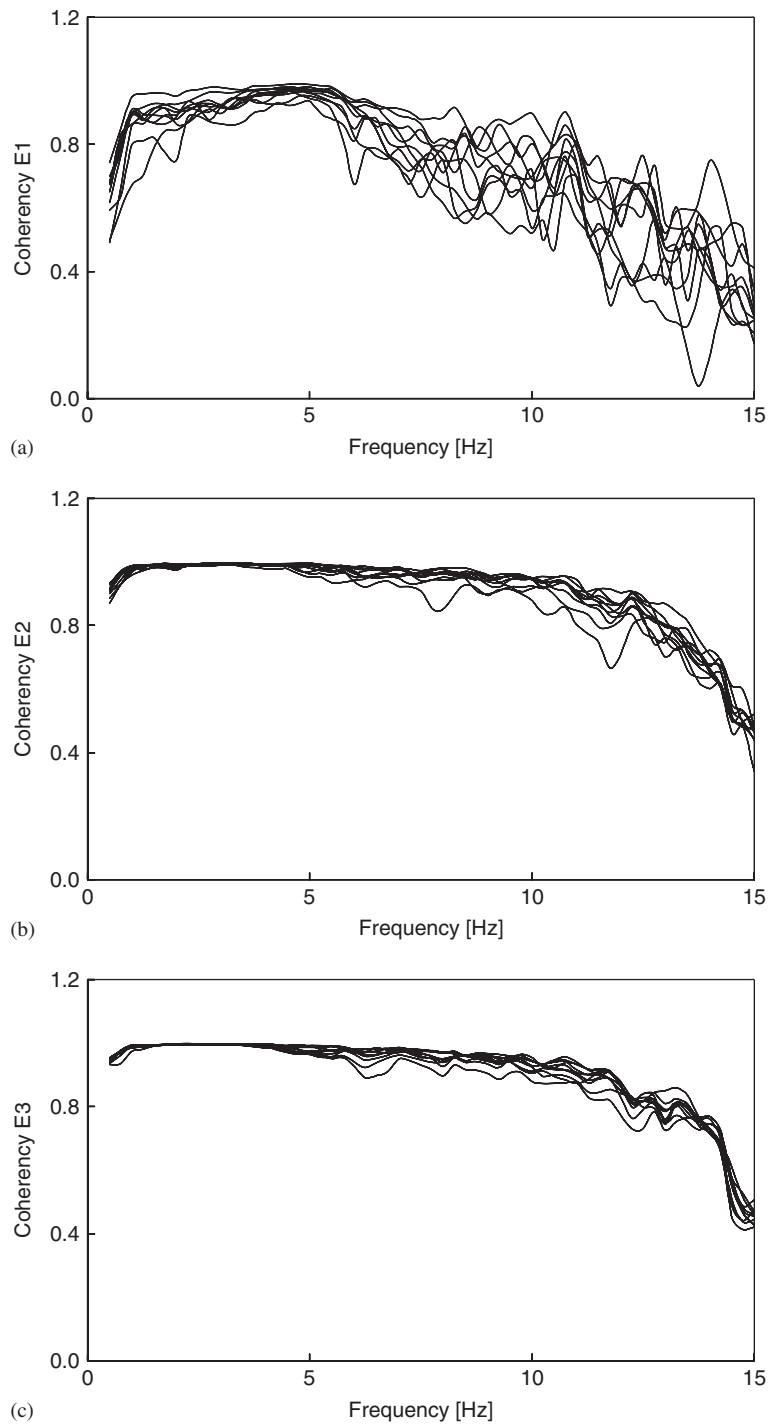


Fig. 8. Individual coherency functions associated with apparent mass functions: (a) during the vibration magnitude E1, (b) during the vibration magnitude E2, (c) during the vibration magnitude E3.

characteristics of the new measurements. The peak frequencies of the apparent mass functions were shown to decrease with the increasing vibration magnitude [2,5,6,13]. This result was confirmed by the apparent mass functions derived from the pressure distribution measurements. The mean peak frequency decreased from 5.25

Table 3

Results of the Bonferroni post hoc test to test the significance level of the differences between the mean values for the three levels of the factor vibration magnitude for the soft seat and the rigid seat

Conditions tested	max $ AM $			$f(\max AM)$		
	E1/E2	E1/E3	E2/E3	E1/E2	E1/E3	E2/E3
Soft seat						
Peak 1	n	.004*	n	.007	.000*	.001*
Peak 2	n	n	n	.000*	.000*	.000*
Rigid seat						
Main peak	n	n	n	.001*	.000*	.000*

(Peak moduli of the apparent masses (max $|AM|$) and peak frequencies ($f(\max|AM|)$) with the magnitudes E1, E2, and E3 for the soft seat as well as magnitudes I1, I2, and I3 for the rigid seat (*—Significance level $p < 0.05$; n—non-significant difference).

Table 4

Forces [N] in z-direction during static conditions: the body weight of the subjects (Body weight), the forces of the upper body acting on the seat cushion (Soft seat) and the forces acting on a rigid seat surface (Rigid seat) during seating without backrest

Subject no.	Body weight	Soft seat Forces seat cushion	Rigid seat Forces seat plate
01	724.0	366.0	528.7
02	845.6	425.0	651.7
03	835.8	395.7	593.7
04	678.9	309.1	506.3
05	725.0	457.0	516.1
06	1016.3	514.1	757.9
07	960.4	567.7	751.2
08	880.0	437.4	751.4
09	663.2	399.4	526.2
10	721.0	335.9	575.3
11	680.8	403.3	533.5
12	601.4	338.9	452.4
13	775.0	405.8	555.9

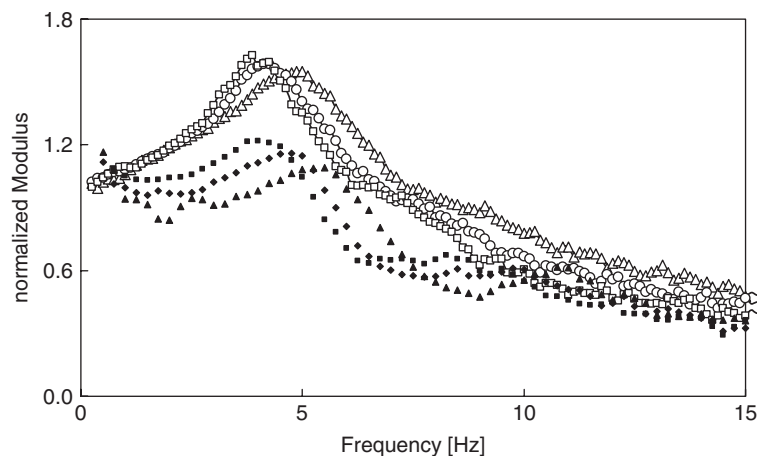


Fig. 9. Normalized mean moduli of the apparent masses calculated by the forces and accelerations measured at rigid seat (AMR): \triangle during the vibration magnitude I1, \diamond during the vibration magnitude I2, \square during vibration magnitude I3, and calculated by the forces and accelerations at the seat cushion (AMS): \blacktriangle during the vibration magnitude E1, \blacklozenge during the vibration magnitude E2, \blacksquare during the vibration magnitude E3.

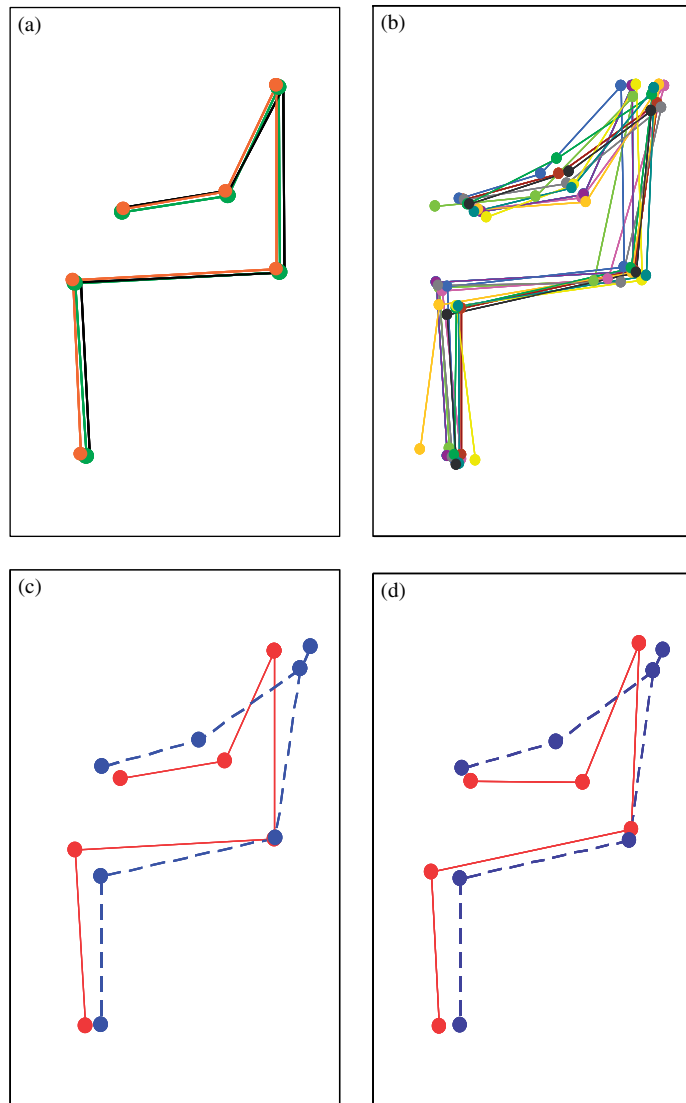


Fig. 10. Stick figures of the subjects: (a) one subject during all conditions tested, (b) all subjects during one condition tested, (c) subjects with extreme body masses, (d) subjects with extreme body heights. ● joint points, ——— maximum body mass (c) and maximum body height (d), - - - minimum body mass (c), minimum body height (d).

to 4.08 Hz (Table 5) during the increase of the vibration magnitude from E1 to E3 by $1.15 \text{ m s}^{-2} \text{ rms}$ (cf. Section 2.3). The mean values of the maximum moduli increased with the vibration magnitude from 48.98 to 53.29 kg—a relatively low difference of 4.31 kg (Table 2).

The experiments using the rigid seat [14] delivered mean peak frequencies in a comparable frequency range: 5.14 Hz during I1 ($0.26 \text{ m s}^{-2} \text{ rms}$) and 4.41 Hz (Table 5) during I3 ($1.57 \text{ m s}^{-2} \text{ rms}$), when the vibration magnitude increased by $1.31 \text{ m s}^{-2} \text{ rms}$ (cf. Section 3.3.2). The mean values of maximum moduli increased with the vibration magnitude from 104.29 to 107.47 kg—the difference of 3.18 kg is in a comparable range to that observed with the soft seat.

The mean values of the normalized moduli of the apparent mass functions for both seating conditions shifted to lower frequencies nearly to the same extent, if the vibration magnitude increased (Fig. 9). The main peak frequencies of AMS and AMR occurred practically in the same range (Table 5). The peak values of the

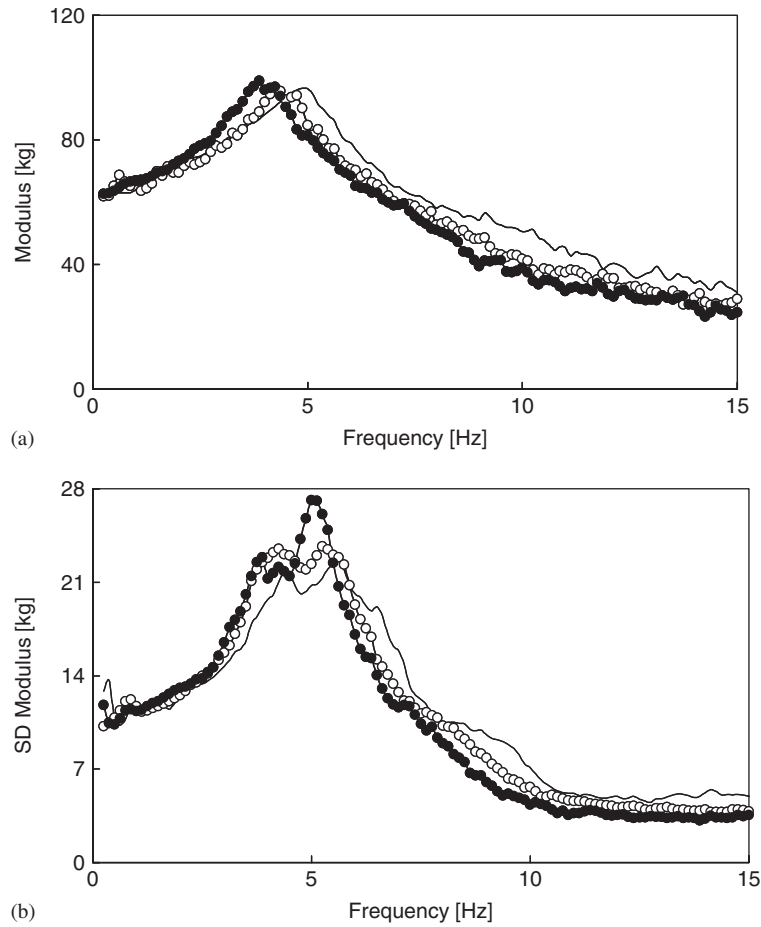


Fig. 11. Moduli of the apparent mass functions calculated by the forces and the accelerations measured at a rigid seat without backrest: (a) mean moduli, (b) standard deviations. — during the vibration magnitude I1, ○ during the vibration magnitude I2, ● during the vibration magnitude I3.

Table 5

Minimum, maximum, and mean values of the peak frequencies of the apparent mass ($f(\max. |AM|)$) determined for soft seat during the vibration magnitudes E1, E2, and E3 and the rigid seat surfaces during the vibration magnitudes I1, I2, and I3

	Seat surface	Minimum (Hz)	Maximum (Hz)	Mean (Hz)
<i>Peak 1</i>				
E1 $f(\max. AM)$	Soft	4.25	6.25	5.25
I1	Rigid	3.38	6.63	5.14
E2 $f(\max. AM)$	Soft	3.75	5.25	4.65
I2	Rigid	3.50	5.88	4.69
E3 $f(\max. AM)$	Soft	3.50	4.75	4.08
I3	Rigid	3.25	5.63	4.41
<i>Peak 2</i>				
E1 $f(\max. AM)$	Soft	8.75	12.25	10.48
I1	Rigid	8.99	10.57	9.78
E2 $f(\max. AM)$	Soft	8.25	10.50	9.48
I2	Rigid	7.82	9.32	8.60
E3 $f(\max. AM)$	Soft	6.75	9.50	8.32
I3	Rigid	6.50	8.25	7.43

second peak of AMS and AMR differed up to a maximum of 0.89 Hz. Slight differences between Fig. 9 and Table 5 were caused by the different methods of averaging: The peak values in the mean curves are the result of averaging individual curves (Fig. 9), the mean peak values in Table 5 were calculated as the average of individual peaks determined for individual curves.

The mean values of the moduli of the apparent masses of the same subjects sitting on a rigid seat (Fig. 11(a)) were remarkably higher than those of the same subjects sitting on the upper part of the driver seat (Fig. 7(a)) and the standard deviations were about twice as much in the range of the main peak (Fig. 11(b), cf. Fig. 7(b)). For a better comparison, normalized values were derived. The differences between the normalized maximum moduli of AMS and AMR are very clear (Fig. 9). It is to consider that different accelerations in *z*-direction were used to calculate the apparent masses: for AMS the acceleration measured at the seat cushion and for AMR the acceleration measured at a rigid seat. The unweighted rms values measured at the seat cushion were slightly higher than those measured at the rigid seat: E1—by 0.03 m s^{-2} , E2—by 0.07 m s^{-2} , and E3—by 0.2 m s^{-2} unweighted rms. These differences are clearly lower than those tested within the studies.

But the power spectral densities as well as the transfer functions showed clearly different patterns of the frequency distributions of the accelerations at the interface between subject and seat surface. A nearly flat spectrum of the acceleration was registered at the rigid seat surface and the plate at which the upper part of the soft seat was mounted (Fig. 1). Peak values in the range between 4 and 6 Hz were found in the power spectral densities of the accelerations at the seat cushion (Fig. 1) and also in the transfer functions (Fig. 4). Since the maximum moduli of the AMR slightly increase with the vibration magnitude, it could be expected that the AMS would be higher in the resonance range of the human body. But opposite results were found.

4.2.2. Backrest and hand support

All studies which tested hand and back supports registered a decrease of the moduli of the apparent mass to a different extent and at different frequencies, depending on the specific experimental design. Apparent masses were derived using rigid seats with and without backrest contact. For tests (vibration intensity 1.0 m s^{-2} rms) with an upright backrest, Towards [10] registered a higher resonance frequency (5.85 Hz) and a lower resonance magnitude (82.0 kg) than for tests without backrest contact (resonance frequency 5.07 Hz, resonance magnitude 99.6 kg). Mansfield and Maeda [12] reported that the apparent mass data for the ‘back-on’ and the ‘back-off’ conditions were similar for many of the subjects (vibration intensity 0.4 m s^{-2} rms). But the median normalized apparent masses had a 5% lower modulus for the ‘back-on’ condition than for the ‘back-off’ condition at frequencies below 3 Hz, whereas between 5 and 10 Hz the median normalized apparent masses were greater for the ‘back-on’ condition than for the ‘back-off’ condition. During a separate test with the same subjects and the same experimental scheme [22] the forces perpendicular to backrest (FX) were in the range between 49 and 125 N (7–20% of the body weight) which indicate a strong dependence on the actual individual posture and considerable variability in spite of identical instructions. Since FX did not correlate with FZ, a significant between-subject variability of the muscle forces contributing to FX may be assumed. Although the backrest contact definitely reduces the force acting on the seat cushion (cf. Section 4.1), the contribution of the backrest contact to this decrease cannot be quantified by the data obtained in this study.

To describe the vibration behaviour better, the measurements of the pressure distribution at the seat and backrest should be performed simultaneously under consideration of the recommendations in Section 4.1 together with a registration of the forces beneath the feet and at the hand support.

4.2.3. Contact conditions at the seat surface

The differences between the pressure distributions of rigid contact areas and soft contact areas were described in detail earlier [17–19]. To test these differences during the vibration exposure, additional tests with subject no. 13 sitting on a rigid seat were performed. Fig. 12 illustrates the results for the exposures I3 (rigid seat, Fig. 12(a)) and E3 (soft seat, Fig. 12(b)). The mean values of the pressure distributions during the vibration exposure exhibited more prominent peak values beneath the buttocks during the test with the rigid seat than with the soft seat. The pressure distributions at the soft seat are a result of the interaction between

the subject and the seat, and may be the reason for certain transfer behaviour of the seat cushion as well as a modified biodynamic behaviour of the human body. From this point of view the interactions between the subject and the seat—reflected in the pressure distributions—and the factors discussed so far—vibration magnitude and backrest contact—may form a complex of reasons, which can not be separated concerning their effects on the apparent mass functions. Since the magnitude can hardly explain the extent of the difference between AMR and AMS (cf. Section 4.2.1), the backrest and different contact conditions of the seat surfaces remain as the probably most important factors.

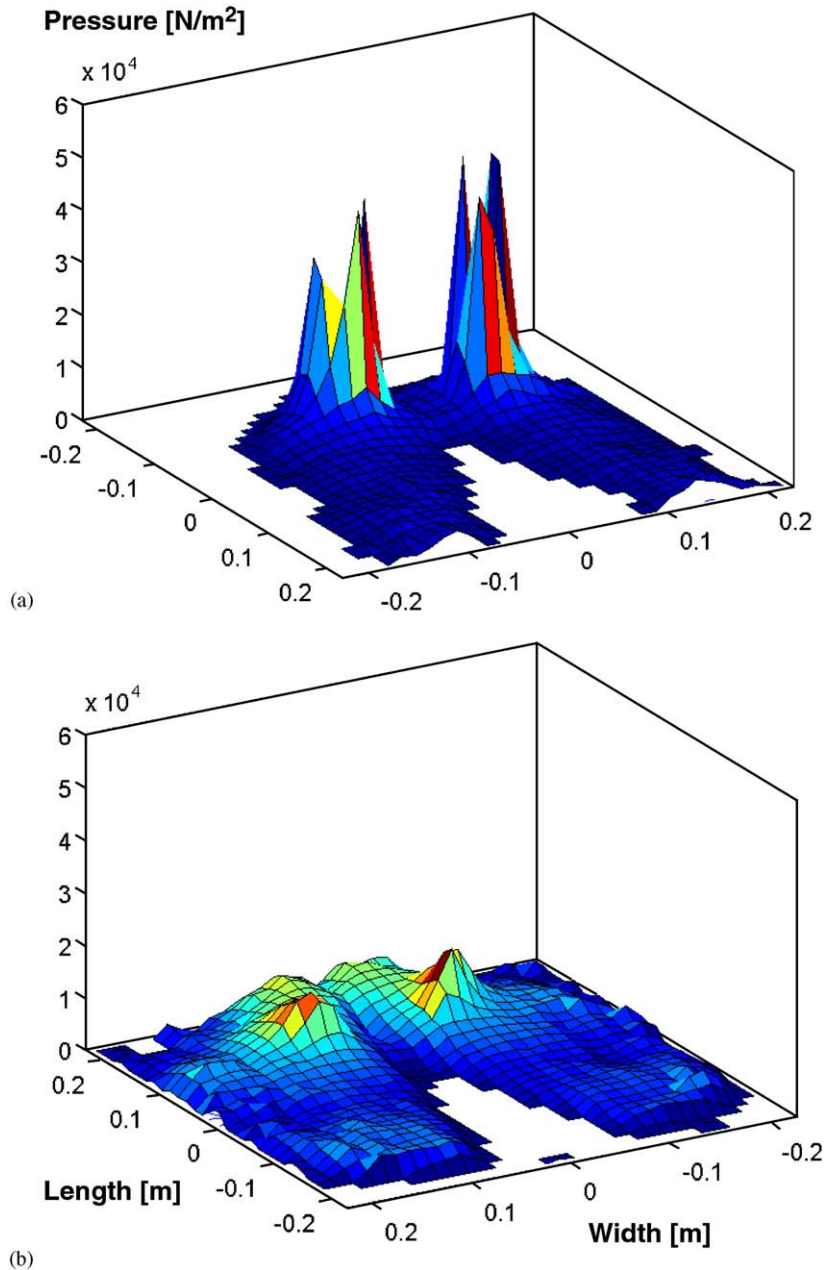


Fig. 12. Results of averaging 1812 individual pressure distributions (subject no. 13) obtained under dynamic conditions: (a) during the vibration magnitude I3 on a rigid seat, (b) during the vibration magnitude E3 on a soft seat cushion.

4.3. Consequences for the modelling

The qualitatively new results could open the possibility to overcome the conventional input condition of models—one point beneath each buttock [11]. From the first experimental results interesting consequences can be derived for the development of biodynamic models: The models for practical conditions should be able to represent the interaction of the human body and the seat. This means that the models should consider a detailed representation of the man–seat-interface. Regarding seating postures models necessarily consist of pliant body parts such as the buttocks, the thighs and the back. The simple approach of one-dimensional connections could be replaced by a more complex geometry which reflects the real body surface.

Further experiments under consideration of the experiences and recommendations of this study could be contributed to a data basis of target functions for an optimization and validation of models considering the soft tissue in contact with a soft seat surface.

5. Conclusions

The results provide for the first time an orientation for the apparent mass functions to be expected under real practical seat conditions, i.e. with various subjects and an upper part of a driver seat with backrest. The quality and profile of the seat surface, the human–seat pressure distribution together with accelerations at the seat cushion, and the backrest contact should be considered as a complex of factors that affects these apparent mass functions.

The data indicate a new quality of target functions for the design and validation of the contact conditions for biodynamic models.

Further studies should be performed under the consideration of the recommended improvements. More research work is needed to confirm the results and to provide a comprehensive data basis for the model development.

Acknowledgements

This study was supported by the German Federal Institute for Occupational Safety and Health in Research Project F2028.

The authors wish to thank for assistance and collaboration Dr. J. Keitel, Dr. M. Schust, and Dipl.-Ing. L. Gericke.

References

- [1] International Organization for Standardization ISO 5982, Mechanical vibration and shock—Range of idealized values to characterize seated-body biodynamic response under vertical vibration, 2001.
- [2] T.E. Fairley, M.J. Griffin, The apparent mass of the seated human body: vertical vibration, *Journal of Sound and Vibration* 22 (1989) 81–94.
- [3] P. Holmlund, R. Lundström, L. Lindberg, Mechanical impedance of the human body in vertical direction, *Applied Ergonomics* 31 (2000) 415–422.
- [4] P.-É. Boileau, X. Wu, S. Rakheja, Definition of a range of idealized values to characterize seated body biodynamic response under vertical vibration, *Journal of Sound and Vibration* 215 (1998) 841–862.
- [5] B. Hinz, H. Seidel, G. Menzel, R. Blüthner, On the variability of the impedance depending on the intensity, posture and body mass, *Zeitschrift für Arbeitswissenschaft* 55 (2001) 7–14.
- [6] B. Hinz, H. Seidel, G. Menzel, L. Gericke, R. Blüthner, J. Keitel, Seated occupant apparent mass in automotive posture—examination with groups of subjects characterised by a representative distribution of body mass and body height, *Zeitschrift für Arbeitswissenschaft* 58 (2004) 250–264.
- [7] N.J. Mansfield, M.J. Griffin, Non-linearities in apparent mass and transmissibility during exposure to whole-body vertical vibration, *Journal of Biomechanics* 33 (2000) 933–941.
- [8] Y. Matsumoto, M.J. Griffin, Non-linear characteristics in the dynamic responses of seated subjects exposed to vertical whole-body vibration, *Journal of Biomechanical Engineering* 124 (2002) 527–529.
- [9] S. Rakheja, I. Stiharu, P.-É. Boileau, Seated occupant apparent mass characteristics under automotive postures and vertical vibration, *Journal of Sound and Vibration* 253 (2002) 57–75.

- [10] M.G.R. Toward, Apparent mass of the seated human body in the vertical direction: effect of holding a steering wheel. *Proceedings of the 39th United Kingdom Group Meeting on Human Response to Vibration*, Ludlow 15–17 September 2004, pp. 211–221.
- [11] J. Hofmann, S. Pankoke, H.P. Wölfel, Individualised FE-model of seated humans and representation of motion segments of the lumbar spine as substructure to determine internal loads during vibration excitation. Research Report Fb 994, FIOSH (Ed.) Wirtschaftsverlag NW, Bremerhaven, 2003.
- [12] N.J. Mansfield, S. Maeda, Effect of backrest and torso twist on the apparent mass of the seated body exposed to vertical vibration, *Industrial Health* 43 (2005) 413–420.
- [13] B. Hinz, S. Rützel, J. Keitel, G. Menzel, H. Seidel, The determination of the apparent mass using car seats as a basis for models of seated men—results of male and female subjects, VDI Reports 1841—Human Vibration, 2004, pp. 57–86.
- [14] B. Hinz, R. Blüthner, G. Menzel, S. Rützel, H. Seidel, H.P. Wölfel, Apparent mass of seated men—determination with single-axis and multi-axes excitations at different magnitudes. *Journal of Sound and Vibration* 2006, in press, doi:10.1016/j.jsv.2006.06.020.
- [15] W. Wang, S. Rakheja, P.-É. Boileau, Effects of sitting postures on biodynamic response of seated occupants under vertical vibration, *International Journal of Industrial Ergonomics* 34 (2004) 289–306.
- [16] N. Nawayseh, M.J. Griffin, Non-linear dual-axis biodynamic response to vertical whole-body vibration, *Journal of Sound and Vibration* 268 (2003) 503–523.
- [17] B. Hinz, L. Gericke, J. Keitel, G. Menzel, H. Seidel, Study of human-seat interface pressure distribution depending on seat type, postures, and anthropometric characteristics, *Zeitschrift für Arbeitswissenschaft* 54 (2002) 159–177.
- [18] B. Hinz, H. Seidel, G. Menzel, J. Keitel, L. Gericke, Laboratory study on pressure distributions at car seats—examination with groups of subjects characterised by a representative distribution of body height and weight, *Zeitschrift für Arbeitswissenschaft* 57 (2003) 169–187.
- [19] X. Wu, S. Rakheja, P.-É. Boileau, Study of human-seat interface pressure distribution under vertical vibration, *International Journal of Industrial Ergonomics* 21 (1998) 433–449.
- [20] International Organization for Standardization ISO 13090, Mechanical vibration and shock—Guidance on safety aspects of tests and experiments with people—part 1: Exposure to whole-body mechanical vibration and repeated shock, 1998.
- [21] B. Hinz, G. Menzel, R. Blüthner, H. Seidel, L. Gericke, M. Schust, Biological effects of typical operating whole-body vibration using real operator seat conditions. Research report 10.004, Editor: FIOSH, Wirtschaftsverlag NW, Bremerhaven, 1996.
- [22] B. Hinz, R. Blüthner, H. Seidel, G. Menzel, Apparent mass functions of the combination subject-seat—an experimental study. Final Report WP3 Annex 1 of the EU-Project VIBSEAT, 2005.
- [23] B. Hinz, H. Seidel, G. Menzel, J. Keitel, L. Gericke, Study of human-seat interface pressure distribution on car seats, *Clinical Biomechanics* 18 (2003) S3–S4.
- [24] A. Kalpen, Personal Communication, 2002.